IRAQI Academic Scientific Journals
Samarra Journal of Pure and Applied Science
SJPAS
www.sjpas.com
p ISSN: 2663-7405
e ISSN: 2789-6838

New Ligand-Based Metal Complexes: Synthesis, Spectroscopic Characterization, Thermal Behavior, Anticancer Properties, and Biological Activity

Mohammed A. Mudhi[1], Enass J. Waheed[2*], Maha Salih Hussein[1]

1 Department of Chemistry, College of Education, University of Samarra, Samarra, Iraq.

2 Department of Chemistry, College of Education for Pure Sciences, Ibn -Al-Haitham, University of Baghdad, Baghdad, Iraq.

https://doi.org/10.54153/sjpas.2023.v5i2.543

Article Information

Received: 27/04/2023
Accepted: 31/05/2023

Keywords:

N^1,N^4-dicarbamothioylsuccinamide, 2-aminobenzothiazole, benzylamine

Corresponding Author

E-mail:
enass.j.w@ihcoedu.uobaghdad.edu.iq
https://orcid.org/0000-0002-4051-0107
Mobile:

Abstract

New ligands, N1, N4-bis (benzo[d]thiazol-2- ylcarbamothioyl) succinamide (L^1) and N1, N4- bis (benzylcarbamothioyl)succinamide (L^2), derived from succinyl chloride and 2-amino benzothiazole or benzylamine, respectively, have been used to prepare a set of transition metal complexes with the general formula $[M_2(L)Cl_4]$, where L=L^1 or L^2, M = Mn(II), Ni(II), Cu(II), Cd(II), Co(II), Zn(II) or Hg(II). The synthesized compounds are characterized using various analytical techniques including TGA, ^{13}C NMR, mass spectroscopy, ^1H and Fourier-transform infrared (FTIR) spectroscopy, magnetic measurement, molar conductivity, electronic spectrum, (%M, %C, %H, %N) and atomic absorption flame (AAF) analysis. The results show that (L^1, L^2) bind to the metal ion in a bidentate fashion through the (C=O) and (C=S) groups, and the complexes have a tetrahedral geometry. The antibacterial activity of the compounds is tested against two types of bacteria, Escherichia coli (−) and Staphylococcus aureus (+). Additionally, the anticancer activity of the Cu(II) and Co(II) complexes was evaluated by carrying out cell viability and cytotoxicity assays on the MCF-7 breast cancer cell line and comparing the results with those obtained for normal cells.

Introduction

In chemistry study, a compound is known as cyclic (or ring) compound in the case where one or more series of its atoms are linked together in order to form a ring. In addition to that, rings could be ranging in their sizes from 3 to many atoms, and the cases where all atoms are carbon are referred to as the carbocycles, whereas others include non-carbon as well as carbon atoms that are present are called as the heterocyclic compounds [1,2].

One of the most significant heterocyclic compounds is benzothiazole, which has great efficacy as a variety of anti-biotic, antimicrobial, anti-fungal, anti-inflammatory, anti-oxidant, analgesic, diuretic, schistosomiasis, and fungicides in wood, geysers in the pulp and paper industry, skin production, chemotherapy, and pesticides [3]. The importance of 2-aminobenzothiazole in the medical area could be attributed to its uses in organic and medical biochemistry, drug discovery, and the creation of medications for the treatment of viral

infections, epilepsy, diabetes, autonomic sclerosis, and tuberculosis. In behavioral, biochemical, and electrophysiological studies, polyfunctional ligands of 2-amino benzothiazoles investigated as a central muscle relaxant were shown to obstruct glutamate neurotransmission [4].

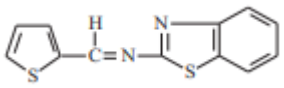
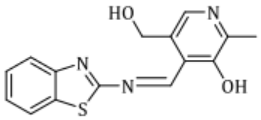

One of the most significant amines, benzoylamine is utilized for producing a variety of organic fine chemicals and medicinal molecules. In the commercial manufacturing of numerous medications, it is a frequent precursor in organic chemistry [5,6]. Due to their intriguing physicochemical characteristics and strong pharmacological and biological effects, metal complexes of S and N chelating ligands had received a lot of attention.

The coordination of the metals in active sites of different metallo bio-molecules is greatly aided by the N and S atoms. Copper, cobalt, zinc, and nickel are some metal ions that could be employed and are frequently utilized since they produce low molecular weight complexes and are thus more effective against a variety of diseases [7,8]. The objective of this study is to determine the structure and geometry of L1 and L2 and their corresponding complexes with $Mn^{(ii)}$, $Ni^{(ii)}$, $Cu^{(ii)}$, $Co^{(ii)}$, $Cd^{(ii)}$, $Hg^{(ii)}$ and $Zn^{(ii)}$ ions.

Chemicals and devices

All analytical and chemical reagents have been purchased from commercial sources and used directly. The numerous chemicals, solvents and metal salts that were employed in this research have been bought from (USA, Sigma-Aldrich, Merck, and India). The equipment (Shimadzu 8400s FT-IR) and CsI disc were used to measure infrared spectroscopy within the range (200-4000 cm-1). The melting point of compounds which were synthesized in an open tube was ascertained using electro-thermal melting point instrument (SMP-10 Stuart). Electron spectra of produced compounds have been examined with the use of (Shimadzu UV1800) visible UV spectrophotometer with concentration of 10^{-3}M samples in the DMSO solvent at the temperature of the room and 1cm quartz cell length. Chemical displacements were captured with the use of the tool (Bruker 300MHz NMR spectrometer) in NMR spectra (^{1}H & ^{13}C). (DMSO-d6 with TMS). %M in complexes is calculated with the use of a Shimadzu (AA 680) equipment.

The molar conductivity of synthesized compounds has been measured at room temperature with the use of conductivity meter - Philips pw-Digital at 10^{-3} M in Dimethyl sulfoxide. The magnetic sensitivity balance (Sherwood Scientific) was used to measure the (μeff B.M) of complexes at room temperature. The prepared compounds' (%C, %H, %N) were calculated with the use of a device called Euro EA 300. TGA-DSC was carried out using a STA PT-1000 Linseis at a temperature range of 0^{o}-1000^{o}C and argon gas.

The Organic Compound

- Synthesis of ligand (L^1 and L^2) [9, 10]

Step A

In the dry acetone (20ml), potassium thiocyanate (0.25g, 2.57mmol) has been dissolved. The first solution was given a gradual addition of succinyl chloride (0.14ml, 0.2g, 1.3mmol)

while being stirred at room temperature for an hour then potassium chloride was removed as a white precipitate by filtration.

StepB

In $(CH_3)_2CO$ (dry) (15ml), 2 -aminobenzothiazole (0 .38g, 2 .5mmol) or benzylamine (0.27 g, 2.5mmol) are dissolved and added after that to solution that has been taken from step A with the stirring and refluxed at 50°-55°C for 3hr-5hr after which this solution has been left at the temperature of the room for 1 hr Then, crashed ice used to cool the solution until precipitate appeared. Has been left to a point where a precipitate appeared**,** see scheme 1.

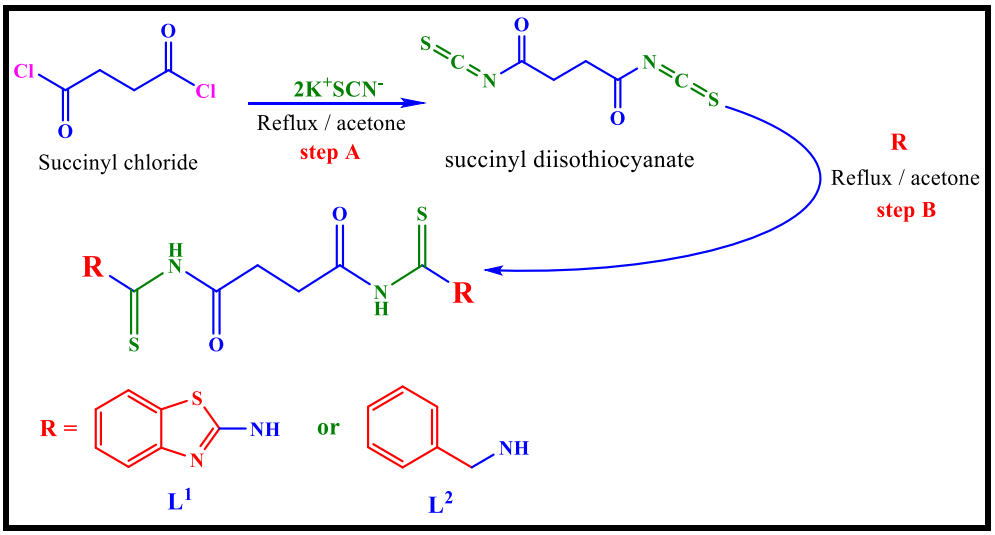

Scheme 1: Preparation course of the (L^1 and L^2)

Synthesis of the complexes

- Synthesis of $[Cu_2(L^1 or L^2)Cl_4]$ complex

Complexes have been prepared in (M: L^1 or L^2) (2: 1) molar ratio. Ethanol solution (10ml) of metal chloride ($CuCl_2.2H_2O$) (0.07gm, 0.4mmol) or (0.08gm, 0.48mmol) has been added into ethanol solution (10ml) of ligand (L^1 or L^2) (0.1gm, 0.2mmol) or (0.1gm, 0.24mmol). This mix has been left at 70°C with continuous stirring and reflex for duration of (3hrs-4hrs). Precipitate with a color Light green or dark green has been formed. This precipitate has been filtered, washed multiple times by diethyl ether and distilled water, then re-crystallized with the use of the absolute ethanol.

- Synthesis of $[M_2(L^1 or L^2)Cl_4]$ complexes

The approach that has been utilized for the preparation of these complexes had been similar to the method that was explained in compound $[Cu_2(L^1 or L^2)Cl_4]$ preparation in the section (II)., obtained solution complex with $Mn^{(ii)}$, $Ni^{(ii)}$, $Co^{(ii)}$, $Cd^{(ii)}$, $Hg^{(ii)}$ and $Zn^{(ii)}$ washed several times with diethyl ether and the distilled water, then re-crystallized with the use of the absolute ethanol**,** see scheme 2.

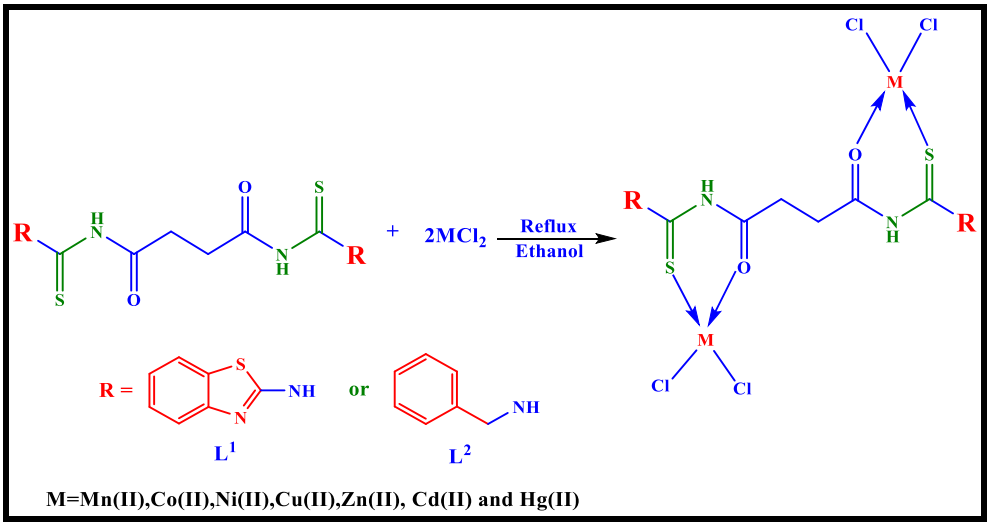

Scheme2: Proposed structure for (L^1 and L^2) complexes.

Results and Discussion

The prepared metal complexes' most crucial properties are their thermal stability and the makeup of colored solid. Soluble in (DMSO) and (DMF) as solvents. For all prepared complexes, practical and theoretical data of (A.A) measurements were approximations, tables 1, 2.

Table1: The physical characteristics of L^1 and its complexes.

Com.	M.wt g / mol	m.pº C or dec.	Color	Microanalysis found (calc.) %					
				M	C	H	N	S	Cl
L^1	500.63	184-186	Brown	------	47.99 (47.98)	3.42 (3.22)	16.68 (16.79)	25.67 (25.62)	------
$[Mn_2(L^1)Cl_4]$	752.30	>300	Brown	14.65 (14.61)	31.81 (31.93)	2.21 (2.14)	11.19 (11.17)	17.15 (17.05)	18.63 (18.85)
$[Co_2(L^1)Cl_4]$	760.29	151-153	Bluish green	15.42 (15.50)	31.67 (31.60)	2.15 (2.12)	11.25 (11.05)	16.89 (16.87)	18.55 (18.65)
$[Ni_2(L^1)Cl_4]$	759.81	>300	Brown	15.35 (15.45)	31.51 (31.62)	2.14 (2.12)	11.12 (11.06)	16.91 (16.88)	18.73 (18.66)
$[Cu_2(L^1)Cl_4]$	769.52	204-206	Dark olive	16.54 (16.52)	31.25 (31.22)	2.13 (2.10)	10.96 (10.92)	16.52 (16.66)	18.51 (18.43)
$[Zn_2(L^1)Cl_4]$	773.19	108-110	Brown	16.79 (16.91)	31.12 (31.07)	2.20 (2.09)	10.76 (10.87)	16.53 (16.59)	18.31 (18.34)
$[Cd_2(L^1)Cl_4]$	867.25	>300	Brown	25.95 (25.92)	27.73 (27.70)	1.88 (1.86)	9.72 (9.69)	14.88 (14.79)	16.40 (16.35)
$[Hg_2(L^1)Cl_4]$	1043.61	155-157	Brown	38.47 (38.44)	23.11 (23.02)	1.58 (1.55)	8.17 (8.05)	12.31 (12.29)	13.62 (13.59)

Table 2: The physical characteristics of L^2 and its complexes.

Com.	M.wt g / mol	m.pºC or dec.	colour	Microanalysis found (calc.) %					
				M	C	H	N	S	Cl
L^2	414.54	112-115	Off white	------	57.83 (57.95)	5.37 (5.35)	13.49 (13.52)	15.44 (15.47)	------
$[Mn_2(L^2)Cl_4]$	666.22	>300	Off white	16.43 (16.49)	36.09 (36.06)	3.39 (3.33)	8.45 (8.41)	9.64 (9.62)	21.31 (21.28)
$[Co_2(L^2)Cl_4]$	674.21	180-182	Blue	17.52 (17.48)	35.68 (35.63)	3.33 (3.29)	8.36 (8.31)	9.55 (9.51)	21.07 (21.03)
$[Ni_2(L^2)Cl_4]$	673.73	>300	Green	17.48 (17.42)	35.69 (35.66)	3.36 (3.29)	8.38 (8.32)	9.57 (9.52)	21.09 (21.05)
$[Cu_2(L^2)Cl_4]$	683.43	215-217	Light olive	18.63 (18.60)	35.20 (35.15)	3.28 (3.24)	8.23 (8.20)	9.42 (9.38)	20.82 (20.75)
$[Zn_2(L^2)Cl_4]$	1101.64	176-178	Off white	19.16 (19.03)	43.72 (43.61)	4.08 (4.03)	10.27 (10.17)	11.67 (11.64)	12.89 (12.87)
$[Cd_2(L^2)Cl_4]$	781.16	>300	Off white	28.79 (28.78)	30.78 (30.75)	2.86 (2.84)	7.27 (7.17)	8.26 (8.21)	18.17 (18.15)
$[Hg_2(L^2)Cl_4]$	957.52	174-176	Off white	41.94 (41.90)	25.13 (25.09)	2.33 (2.32)	5.87 (5.85)	6.72 (6.70)	14.84 (14.81)

Mass spectral

Fragmentation of the mass spectral data of (L^1), figure 1-A showed ((M^+=500.6) (25%) and chemical formula $[C_{20}H_{16}N_6O_2S_4]$. While data fragmentation of the mass spectra of L^2, figure1-B showed (M^+=414.5) (21.25%) and chemical formula $[C_{20}H_{22}N_4O_2S_2]$ [11,12]. Additional fragmentation is displayed in table 3.

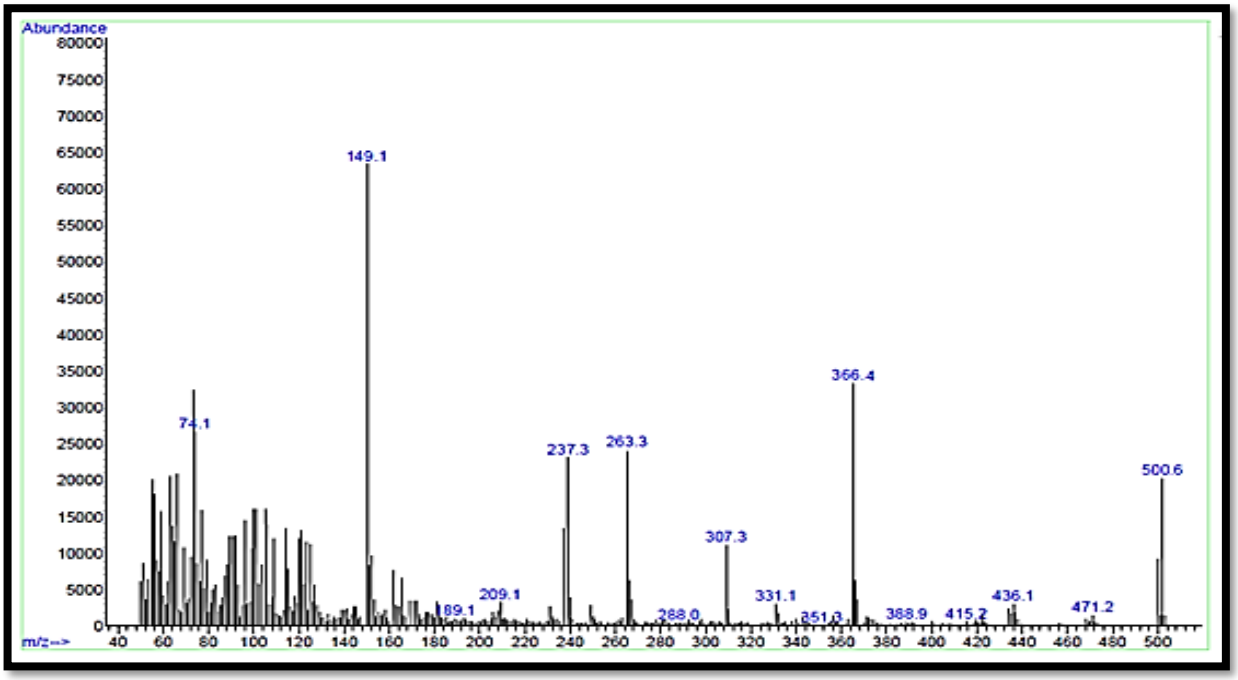

Fig. 1-A: Mass spectrum of L^1

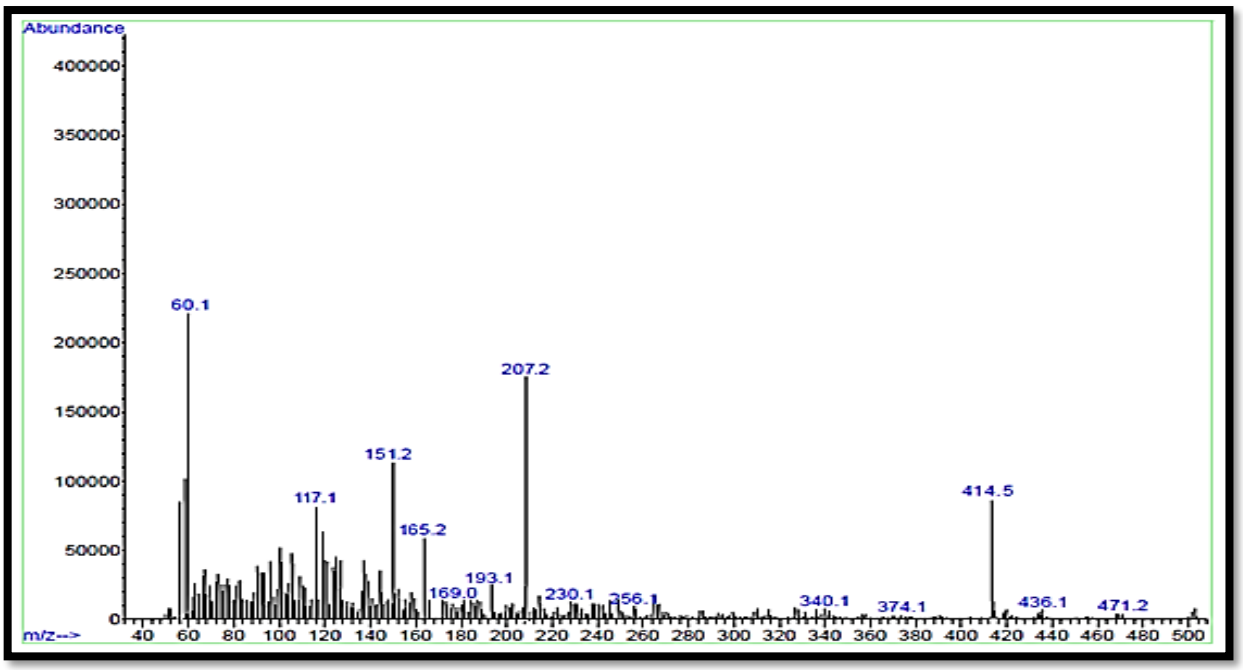

Fig. 1-B: Mass spectrum of L^2

Table 3: The data of mass spectra (L^1 and L^2)

Ligand fragment (L^1)	Mass/charge (m / z)	(%) Relative Abundance	Ligand fragment (L^2)	Mass/charge (m/z)	Relative Abundance (%)
$[C_{20}H_{16}N_6O_2S_4]^{\cdot+}$	500.63	25	$[C_{20}H_{22}N_4O_2S_2]^{\cdot+}$	414.54	21.25
$[C_{13}H_{12}N_5O_2S_3]^{\cdot+}$	366.45	42.5	$[C_{10}H_{11}N_2OS]^{\cdot+}$	207.27	43.75
$[C_{12}H_{11}N_4O_2S_2]^{\cdot+}$	307.37	13.75	$[C_8H_9N_2S]^{\cdot+}$	165.23	15
$[C_{11}H_9N_3OS_2]^{\cdot+}$	263.33	30	$[C_8H_9NS]^{\cdot+}$	151.23	28.75
$[C_9H_7N_3OS_2]^{\cdot+}$	237.30	28.75	$[C_3H_5N_2OS]^{\cdot+}$	117.15	21.25
$[C_8H_6N_2S_2]^{\cdot+}$	194.27	13.75	$[CH_2NS]^{\cdot+}$	60.09	52.2
$[C_7H_5N_2S]^{\cdot+}$	149.19	80	$[C_2H_4NO]^{\cdot+}$	58.06	21.25
$[CH_2N_2S]^{\cdot+}$	74.10	33.75	$[C_4H_8]^{\cdot+}$	56.11	21.25

NMR Spectra

^{1}H-NMR Spectra of (L^1 & L^2)

An integral intensity of each signal in the 1HNMR spectra of (L1, L2), figure 2-(A ,B) has been found to be consistent with the number of various groups of the protons presents [13-16], as listed in the table 4.

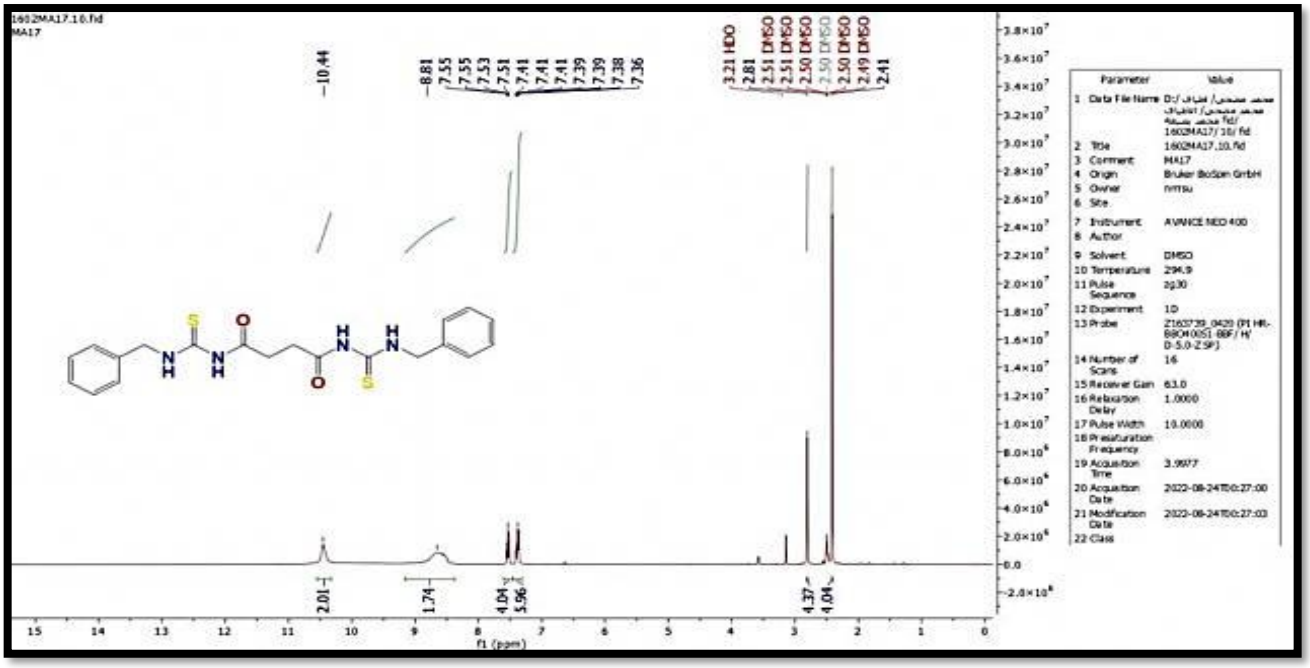

Fig. 2-A: ^{1}H-NMR spectra of (L^{1})

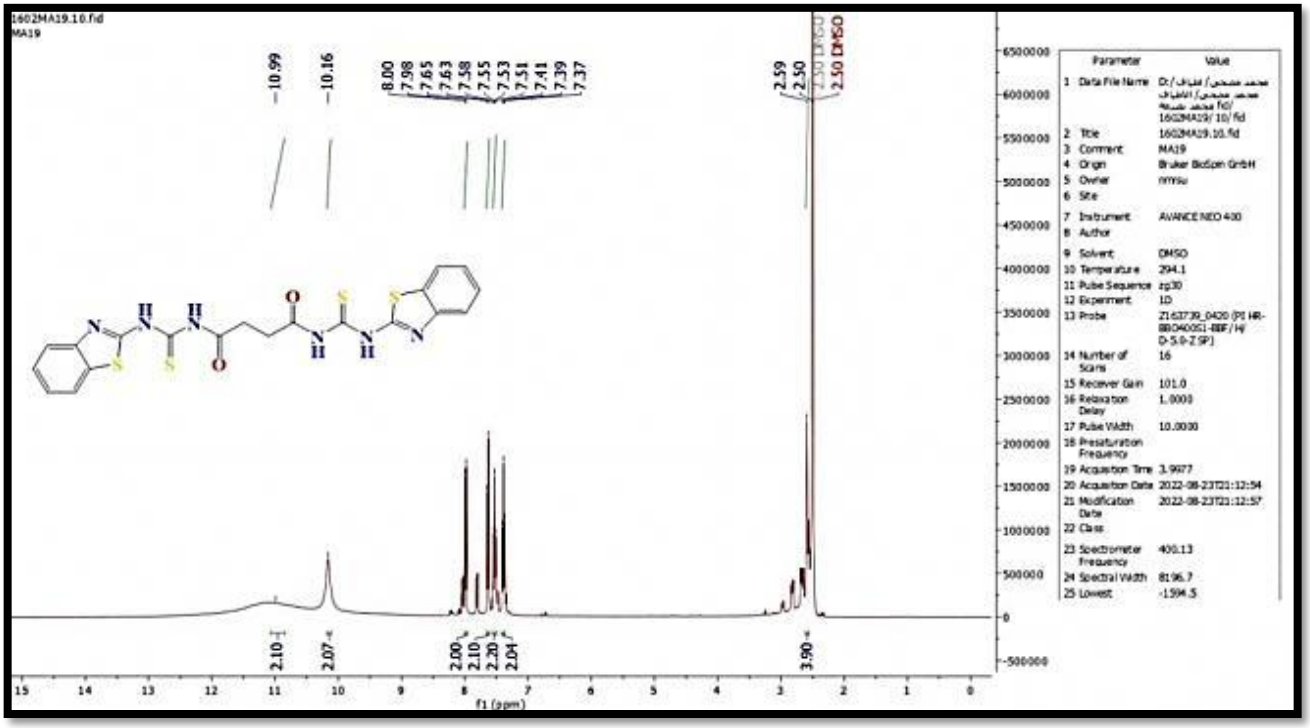

Fig. 2-B: ^{1}H-NMR spectra of (L^{2})

Table4: Chemical shift and NMR data of (L^1) & (L^2)

Ligand	Protons kids	δ (ppm)	Ligand	Protons kids	δ (ppm)
L^1	2 H (-singlate), CSN**H** proton group	10.99	L^2	2 H (singlate), proton CON**H** group	10.44
	2 H (-singlate), CON**H** proton group	10.16		2 H (singlate), proton CSN**H** group	8.81
	8 H (-multiplate), proton aromatic (six ring) from benzothiazole group	7.37-8.00		10H (multiplate), proton aromatic (six ring) from benzyl group	7.55-7.36
	4 H (-triplate), C**H₂** proton group from methylene succinyl group	2.59		4 H (singlate), from methylene benzyl group	2.81
				4 H (triplate), proton C**H ₂** group from methylene succinyl group	2.41
	Dimethyl sulfoxide	2.50		Dimethyl sulfoxide	2.50

^{13}C-NMR Spectra of (L^1 & L^2)

In integrated intensity of each signal in ^{13}CNMR spectra of (L^1, L^2), figure 3-(A,B) was found to be consistent with the number of different groups of carbons presents [17-20], as listed in the table 5.

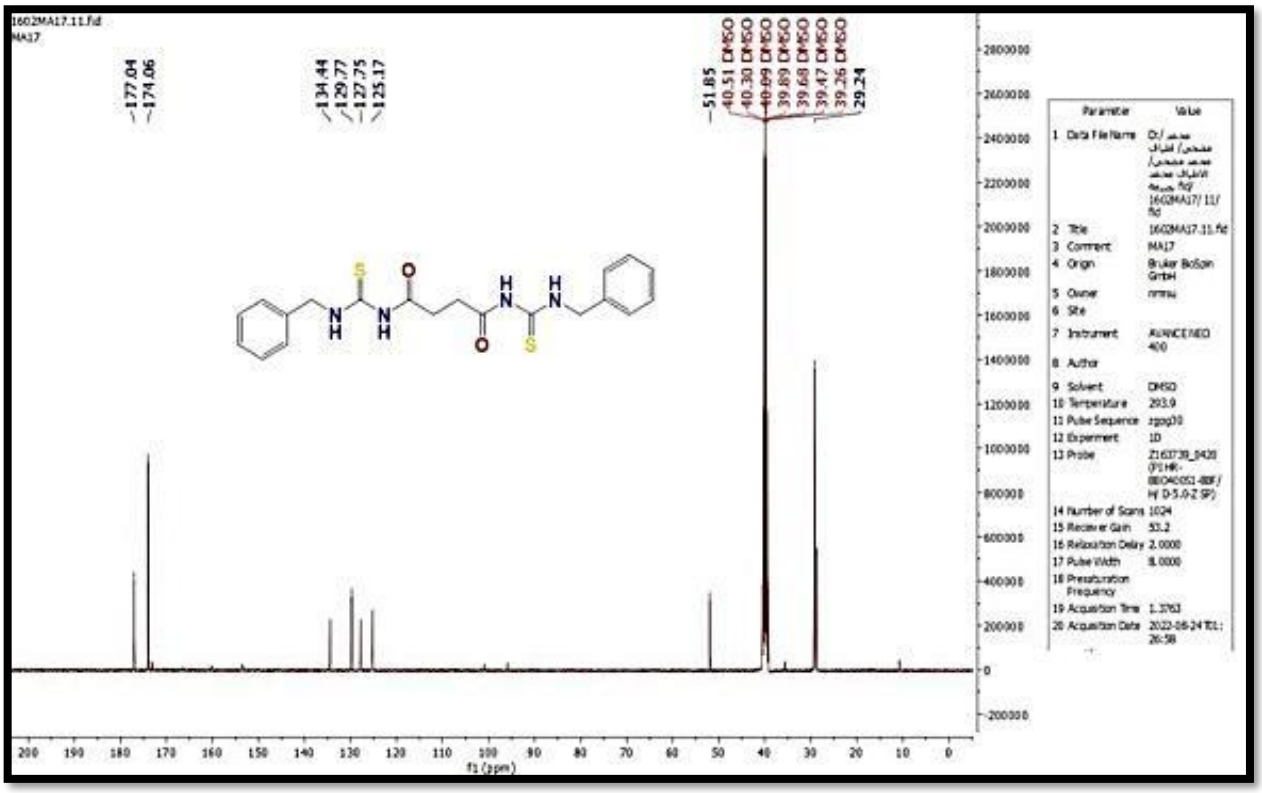

Fig. 3-A: ^{13}C-NMR spectra of (L^1)

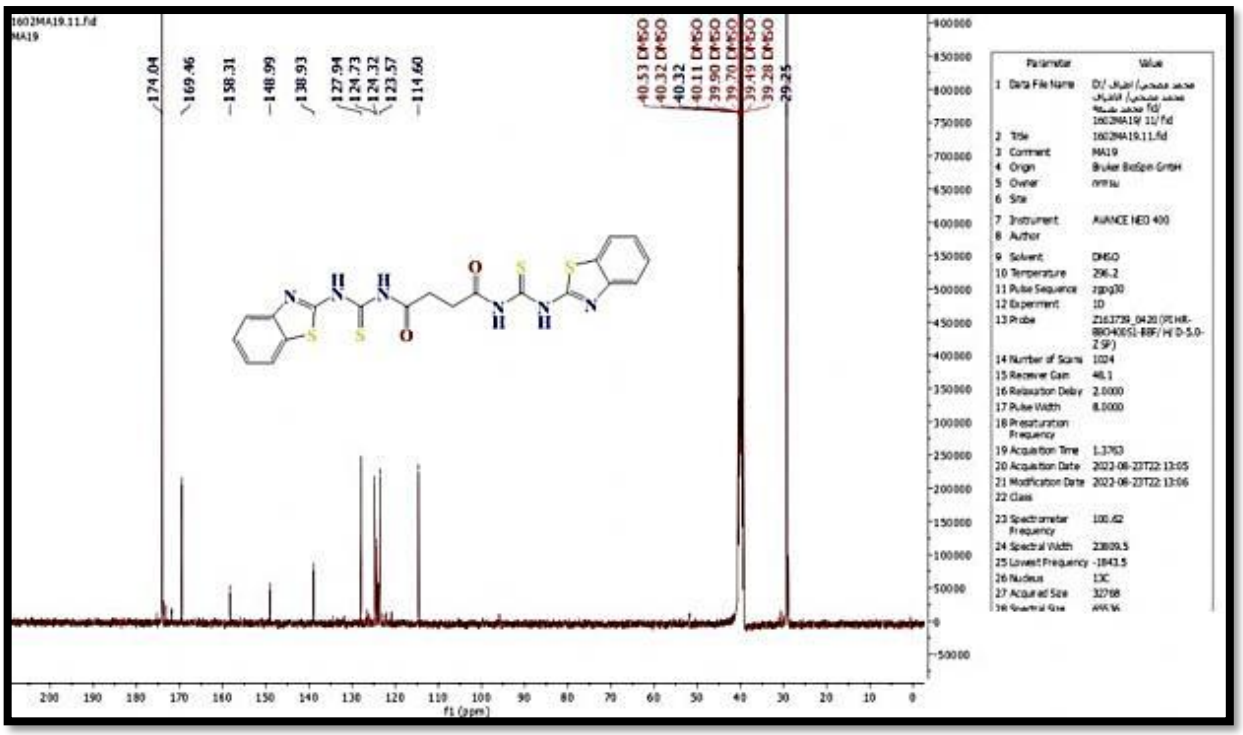

Fig. 3-B: ^{13}C-NMR spectra of (L^2).

Table 5: ^{13}C-NMR data for (L^1) and (L^2) measured in DMSO-d_6 and chemical shifting in ppm.

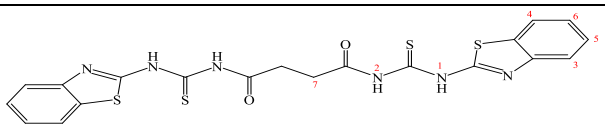

L^1

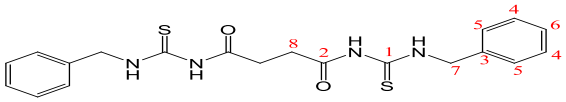

L^2

Ligand	Carbons signals	δ (ppm)	Ligand	Carbons signals	δ (ppm)
L^1	C $_1$ for C=S, thioamide group	174.04	L^2	C_1 for C=S, thioamide group	177.04
	C $_2$ for C=O, amide group	169.46		C $_2$ for C=O, amide group	174.06
	C $_3$ for C=N (in five ring), benzothiazole group	158.31		C $_3$-C_6 for phenyl (six ring), benzyl group	125.17-134.44
	C_4-C_9 for phenyl (six ring), benzothiazole group	148.99-114.60		C_7 for methylene benzyl group	51.85
	C_{10} for (CH_2-CH_2) aliphatic in succinyl group	40.32		C_8 for (CH_2-CH_2) aliphatic in succinyl group	29.24
	DMSO	39.26-40.51		DMSO	39.28-40.53

FT-IR Spectra

Ligand (L^1 and L^2)

The two band at (3470 and 3342) cm^{-1} in L^1 spectrum have been determined to υ (N-H), while added band of a bsorption was exhibited at (1724)cm^{-1} can be expressed as υ $(CO)_{amide}$, also bands of absorption at (1331 & 1138) cm^{-1} that had determined to υ(C=S), and a different absorption band was display at 1257cm^{-1} can be interpreted as υ (C-N) whereas The 2 bands at (3474 and 3378) cm^{-1} in L^2 spectrum that had been determined to υ(NH), while another band of absorption was exhibited at (1732cm^{-1}) can be signified as υ(C=O) amide, in addition to absorption bands at (1342 and 1172cm^{-1}) which had determined to υ(CS) , and added absorption band was exhibited at (1232) cm^{-1} can be expressed as υ (CN) [21,22].

Complexes of ligands (L^1 and L^2)

These spectra had exhibited a considerable difference among bands which be owned by $υ(C=O)_{amide}$ stretch vibration in (1716-1693) cm^{-1} range shifted to different frequency values that propose likelihood of co-ordination of (L^1) by oxygen atom at amide group[18]. Stretching vibration band υ(C=S) was found in a range (1311-1307) and (1176-1161) cm^{-1} shifted to another frequency and that indicates that sulfur atom has been involved in coordination[19]. υ (NH) in (L^1) has not been connected to metal ion and has been established by no variations in the standards of frequency of this group, which have been set at (3475-3411) and (3387-3319) cm^{-1} in complexes. In spectra of complexes, new bands υ(M-S, thioamide group), υ(M-O,amide group) and υ(M-Cl,amide group) appeared in (493-459) cm^{-1}, (559-524) cm^{-1} and (383-329) cm^{-1} respectively. The co-ordination through sulfur atom in group (NH-S=O), oxygen atom in (NH-C=O) group and ion chloride (Cl^-) with metal ions had resulted in appearance of new bands which indicate metal complex formations [23,24]. In table 6, the FTIR data has been shown. In figure 4 (A,B), spectrum of (L^1) and its complexes have been presented.

While these spectra had shown a considerable variations between bands which belong to stretching vibration of υ(CO, amide group) in (1724-1693) cm^{-1} range shifted to various values frequency suggesting probability of co-ordination of (L^2) by O atom at NHCO group. The stretch vibration υ (CS) had been found in range (1396-1307) and (1199-1176) cm^{-1} shifted to another frequency value, and that indicates that sulfur atom has been involved in coordination[19]. υ(N-H) in (L^4) hasn't been correlated with central ion and has been confirmed by no variations in frequency values of this group, which have been set at (3487-3411) and (3429-3318) cm^{-1} in complexes. In complexes spectra, new bands υ(M-O,amide group), υ(M-S, thioamide group), and υ(M-Cl,amide group) appeared in the (497-489), (559-505) and (386-282) cm^{-1} respectively. The co-ordination via S atom in (NHSO) group, O atom in (NHCO) group and ion chloride (Cl^-) with metal ions had resulted in emergence of new bands, indicating metal complex formation [25,26]. In table7, the FTIR data has been shown. In figure 5 (A,B), spectrum of (L^2) and its complexes have been shown.

Table6: FT-IR data of (L^1) (cm^{-1}) and their complexes.

Compounds	υ(N-H)	υ(C=O) Amide	υ(C=S) υ(C=S)	υ(C-N)	υ(M-O)	υ(M-S)	υ(M-Cl)
L^1	3470 3342	1724	1331 1138	1257	———	———	———
$[Mn_2(L^1)Cl_4]$	3477 3387	1693	1311 1176	1284	559	493	362
$[Co_2(L^1)Cl_4]$	3420 3371	1697	1307 1176	1249	524	493	334
$[Ni_2(L^1)Cl_4]$	3414 3338	1697	1307 1176	1257	559	459	329
$[Cu_2(L^1)Cl_4]$	3475 3335	1716	1307 1176	1246	524	493	365
$[Zn_2(L^1)Cl_4]$	3425 3378	1701	1307 1161	1246	543	493	352
$[Cd_2(L^1)Cl_4]$	3438 3319	1693	1311 1176	1284	559	459	364
$[Hg_2(L^1)Cl_4]$	3411 3321	1693	1311 1176	1257	547	459	382

Table 7: FT-IR data of (L^2) (cm^{-1}) and their complexes

Compounds	υ(N-H)	υ(C=O) Amide	υ(C=S) υ(C=S)	υ(C-N)	υ(M-O)	υ(M-S)	υ(M-Cl)
L^2	3474 3378	1732	1342 1172	1232	———	———	———
$[Mn_2(L^2)Cl_4]$	3421 3372	1693	1311 1180	1241	559	489	375
$[Co_2(L^2)Cl_4]$	3479 3429	1701	1307 1176	1241	551	497	282
$[Ni_2(L^2)Cl_4]$	3468 3410	1705	1311 1199	1242	524	489	317
$[Cu_2(L^2)Cl_4]$	3411 3373	1724	1311 1176	1246	559	493	324
$[Zn_2(L^2)Cl_4]$	3487 3318	1705	1396 1192	1246	505	489	298
$[Cd_2(L^2)Cl_4]$	3468 3425	1724	1311 1184	1242	524	489	386
$[Hg_2(L^2)Cl_4]$	3483 3332	1720	1311 1176	1242	524	493	321

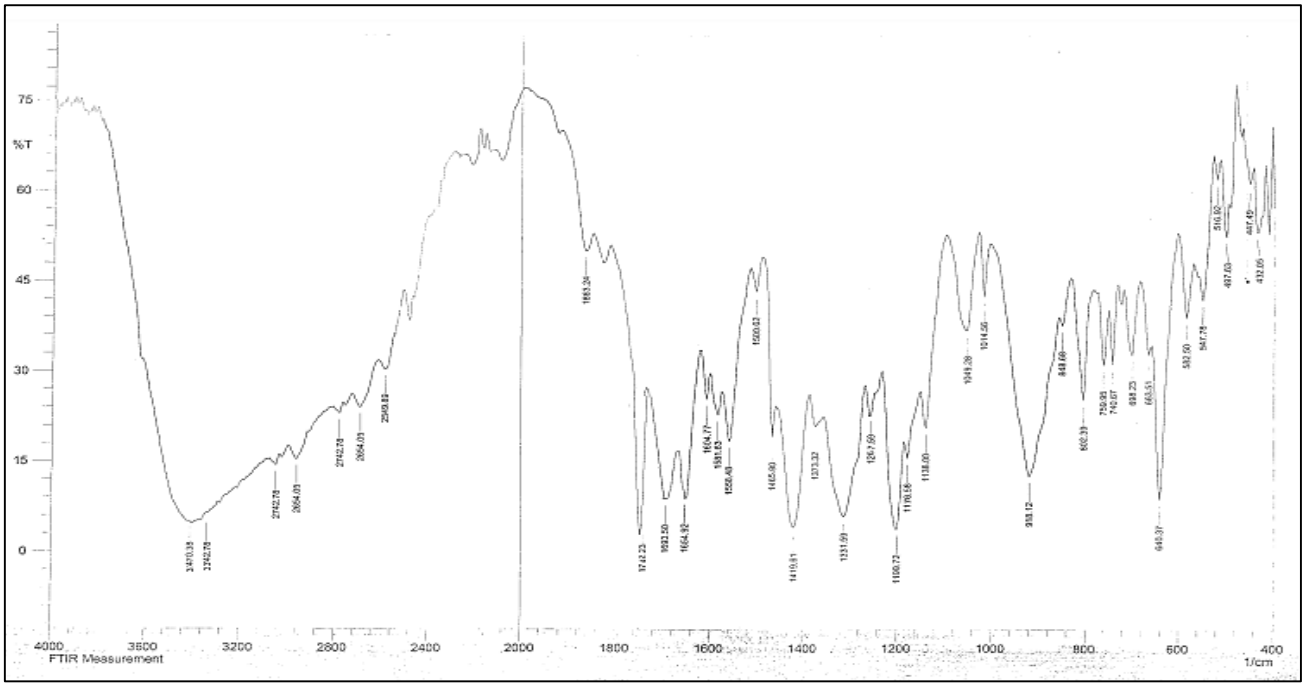

Fig. 4-A: FTIR spectrum of L^1

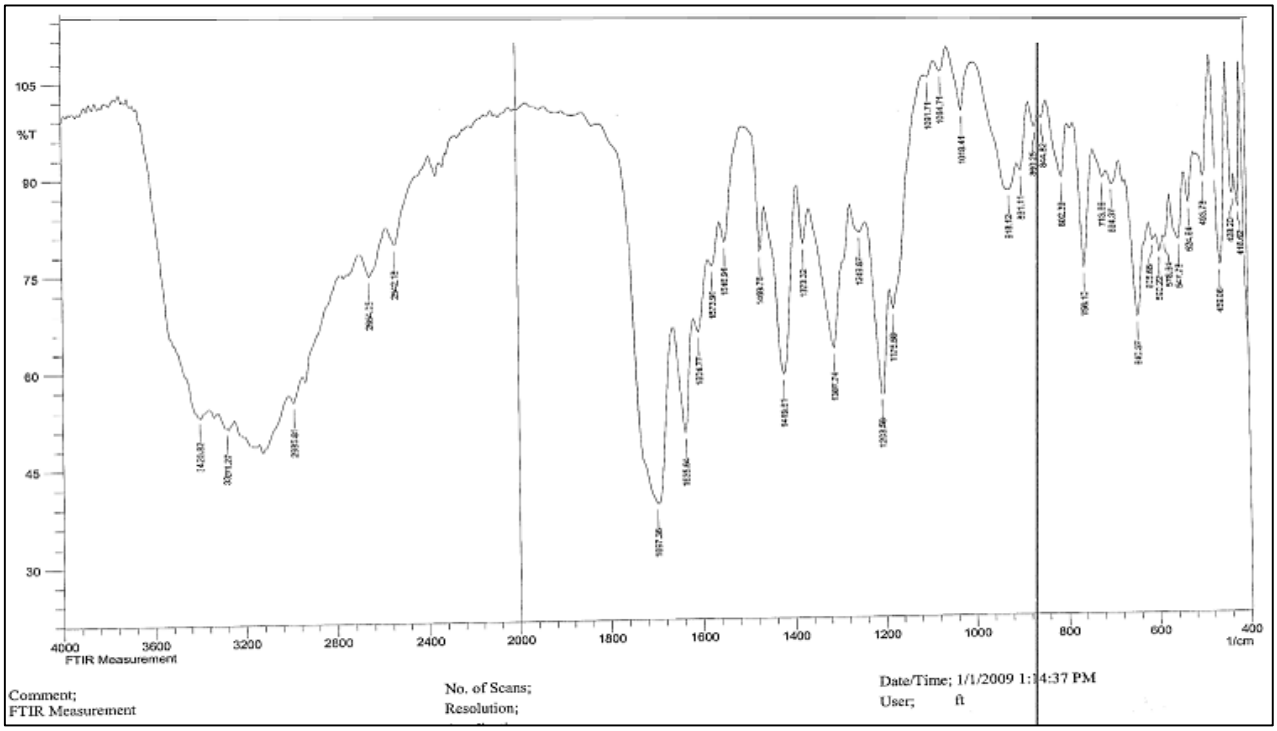

Fig. 4-B: FTIR spectrum of Co-complex

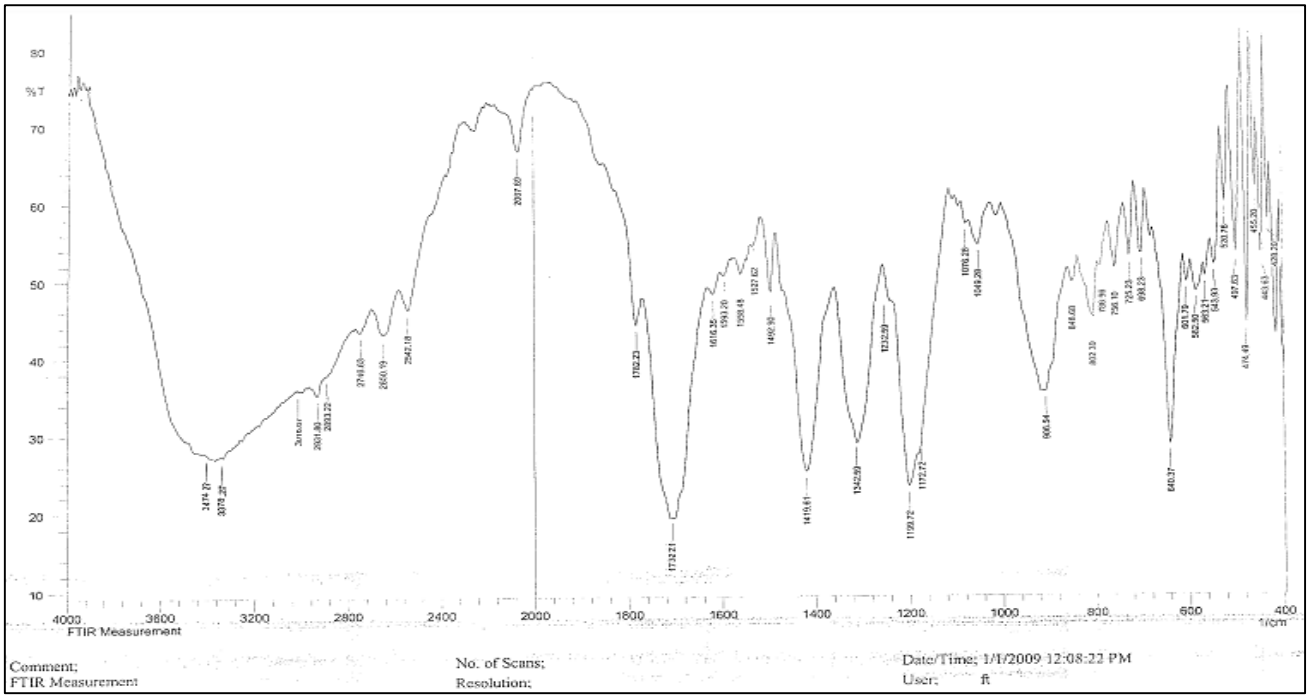

Fig. 5-A: FTIR spectrum of L^2

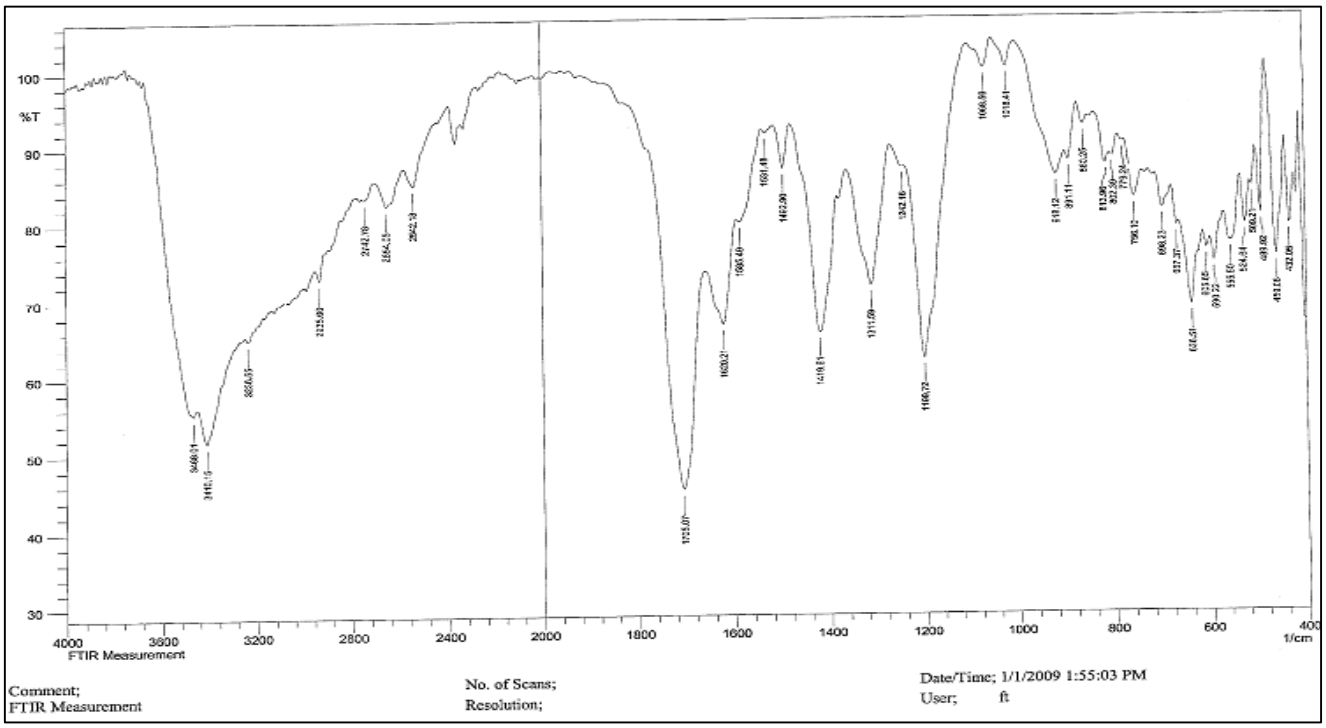

Fig. 5-B: FTIR spectrum of Ni-complex

Electronic spectra

Ligand (L^1 and L^2)

The maximum intensity of absorption has been found at 37037cm $^{-1}$ which results from transitions (π→π*) and at (33333) cm $^{-1}$ which is due to transitions (n→π*) in electronic spectra of (L^1) [27], In table 8 data have been recorded.

While maximum intensity of absorption has been found at 35971cm $^{-1}$ which results from transitions (π→π*) and at (31746) cm $^{-1}$ which is due to transitions (n→π*) in (L^2) electronic spectrum [28], In table 9 data have been recorded.

The Complexes

Ligand (L^1) Complexes / electronic spectrum of manganese complex had shown bands at (36630, 23364 & 13157) cm^{-1} due to the I.L (Intra Ligand), C.T and $^6A_1 \rightarrow {}^4T_{2(G)}$ transition correspondingly, suggesting that it had tetra-hedral structure. Created bands in cobalt complex at (36363, 33333, 25839, 14792 and 10989) cm^{-1}, which is back to L.F, C.T with $^4A_{2(F)} \rightarrow {}^4T_{1(F)}$, $^4A_{2(F)} \rightarrow {}^4T_{1(P)}$ and $^4A_{2(F)} \rightarrow {}^4T_{2(F)}$ transitions, tetra-hedral structure of complex was proposed. About nickel complex, electronic spectra appear absorption bands could be given to I. L, C.T with $^3T_1 \rightarrow {}^3T_{1(P)}$, $^3T_1 \rightarrow {}^3A_{2(F)}$ and $^3T_1 \rightarrow {}^3T_{2(F)}$ transition which exhibit in (36900, 33333, 28169, 12903 and 12150) cm^{-1} respectively. A characterization of these bands is an indication that the complex had tetrahedral geometry. Confirming copper complex's tetrahedral geometry is appearance of bands at (36630, 32786 & 11737) cm^{-1} is returns to I. L and $^2T_2 \rightarrow {}^2E$ transitions. The tetra-hedral structure of zinc complex was suggested on basis of bands which had appeared at (34965, 33333 and 27027) cm^{-1} which is back to L.F, L.F and C.T. based on bands in the mercury complex at (37037, 33333 & 23529) cm^{-1}, which is back to L.F, L.F and C. T transitions respectively, tetra-hedral structure of complex was proposed. The tetra-hedral structure of the cadmium complex had been proposed on a basis of band which had shown at (36496, 33557 and 23529) cm^{-1} which was back to L.F, L.F and C.T [29-31]. In table 8, U.V. data has been shown. In figure 6 (A,B) spectra of the (L^3) and its complexes have been shown.

Ligand (L^2) Complexes/ electronic spectra of manganese complex had shown bands at (36231, 28571 and 12180) cm^{-1} because of the I.L, C.T and $^6A_1 \rightarrow {}^4T_{2(G)}$ transitions correspondingly, which proposes the fact that it had tetra-hedral structure. According to bands in the Cobalt complex at (35971, 26315, 14792 and 11111) cm^{-1}, which returned to L.F, CT with $^4A_2 \rightarrow {}^4T_{1(P)}$, $^4A_{2(F)} \rightarrow {}^4T_{1(F)}$ and $^4A_{2(F)} \rightarrow {}^4T_{2(F)}$ transitions correspondingly, tetra-hedral structure of complex was proposed. Concerning nickel complex, electron spectra appear absorption bands could be assigned to I.L, C.T mix $^3T_1 \rightarrow {}^3T_{1(P)}$, $^3T_1 \rightarrow {}^3A_{2(F)}$ and $^3T_1 \rightarrow {}^3T_{2(F)}$ transition, exhibiting in (35842, 28571, 13333 and 11049) cm^{-1} respectively. Characterization of these bands gives an indication that the complex has tetra-hedral structure. Confirming tetra-hedral structure of copper complex is appearance of bands at (35714, 23809 and 12048) cm^{-1} are returns to I.L, C.T and transitions of $^2T_{2\,(F)} \rightarrow {}^2E$. tetra-hedral structure of zinc complex had been proposed based upon band which had appeared at the values of (36630 and 26315) cm^{-1} which returns to the I. L and C. T. based on bands in Hg complex at (36231 and 25641) cm^{-1}, which returns to the I.L and C.T transitions respectively, tetra-hedral structure of complex was suggested. Tetra-hedral structure of cadmium complex was proposed on a basis of the band which had appeared at (36363 and 26178) cm^{-1} which was back to I. L and C.T [32-34]. In table 9, U.V. data has been shown. In figure 7-(A,B) spectra of (L^2) and its complexes have been shown.

Table 8: Electronic transfers in prepared compounds' spectra.

Compounds	Wave number		A	ε_{max} molar^{-1} cm^{-1}	Transitions	μ_{eff} B.M.	Conductivity Ohm^{-1}cm^{2}mol^{-1} in solvent (DMSO)
	nm	cm^{-1}					
L^1	270 300	37037 33333	2.306 0.480	2306 480	$\pi - \pi^*$ $n - \pi^*$	-	
$[Mn_2(L^1)Cl_4]$	273 428 760	36630 23364 13157	1.773 0.033 0.045	1773 33 45	I.L C.T $^6A_1 \rightarrow {}^4T_{2(G)}$	6.04	19
$[Co_2(L^1)Cl_4]$	275 300 387 676 910	36363 33333 25839 14792 10989	2.209 1.040 0.072 0.056 0.034	2209 1040 72 56 34	I.L C.T $^4A_{2(F)} \rightarrow {}^4T_{1(P)}$ $^4A_{2(F)} \rightarrow {}^4T_{1(F)}$ $^4A_{2(F)} \rightarrow {}^4T_{2(F)}$	4.71	22
$[Ni_2(L^1)Cl_4]$	271 300 355 775 823	36900 33333 28169 12903 12150	2.240 0.954 0.651 0.422 0.050	2240 954 651 422 50	I.L C.T $^3T_1 \rightarrow {}^3T_{1(P)}$ $^3T_1 \rightarrow {}^3A_{2(F)}$ $^3T_{1)} \rightarrow {}^4T_{2(F)}$	3.87	13.5
$[Cu_2(L^1)Cl_4]$	273 305 852	36630 32786 11737	1.691 1.189 0.061	1691 1189 61	I.L I.L $^2T_{2\,(F)} \rightarrow {}^2E$	2.26	15
$[Zn_2(L^1)Cl_4]$	286 300 370	34965 33333 27027	2.130 1.892 0.911	2130 1892 911	I.L I.L C.T	0	13.2
$[Cd_2(L^1)Cl_4]$	274 298 425	36496 33557 23529	1.549 1.173 0.043	1549 1173 43	I.L I.L C.T	0	8.9
$[Hg_2(L^1)Cl_4]$	270 300 425	37037 33333 23529	2.211 1.635 0.062	2211 1635 62	I.L I.L C.T	0	11

I.L=Intra Ligand C.T=Charge transfer

Table 9: Electronic transfers in prepared compounds' spectra.

Compounds	Wave number		A	ε_{max} molar^{-1} cm^{-1}	Transitions	μ_{eff} B.M.	Conductivity Ohm^{-1}cm^{2}mol^{-1} in solvent (DMSO)
	nm	cm^{-1}					
L^2	278 315	35971 31746	1.583 0.034	1583 34	$\pi - \pi^*$ $n - \pi^*$	-	
$[Mn_2(L^2)Cl_4]$	276 350 821	36231 28571 12180	1.923 1.476 0.047	1923 1476 47	I.L C.T $^6A_1 \rightarrow {}^4T_{2(G)}$	5.71	16.1
$[Co_2(L^2)Cl_4]$	278 380 676 900	35971 26315 14792 11111	2.104 0.065 0.090 0.018	2104 65 90 18	I.L $^4A_{2(F)} \rightarrow {}^4T_{1(P)}$ $^4A_{2(F)} \rightarrow {}^4T_{1(F)}$ $^4A_2 \rightarrow {}^4T_{2(F)}$	4.49	18.4

$[Ni_2(L^2)Cl_4]$	279 350 750 905	35842 28571 13333 11049	1.563 0.650 0.036 0.021	1563 650 36 21	I.L $^3T_1 \rightarrow {}^3T_{1(P)}$ $^3T_1 \rightarrow {}^3A_{2(F)}$ $^3T_1 \rightarrow {}^3T_{2(F)}$	3.68	23
$[Cu_2(L^2)Cl_4]$	280 420 830	35714 23809 12048	1.443 0.057 0.072	1443 57 72	I.L C.T $^2T_{2\,(F)} \rightarrow {}^2E$	2.19	7.9
$[Zn_2(L^2)Cl_4]$	273 380	36630 26315	2.419 0.068	2419 68	I.L C.T	0	4.3
$[Cd_2(L^2)Cl_4]$	275 382	36363 26178	2.198 0.043	2198 43	I.L C.T	0	9.3
$[Hg_2(L^2)Cl_4]$	276 390	36231 25641	1.667 0.023	1667 23	I.L C.T	0	12

I.L=Intra Ligand C.T=Charge transfer

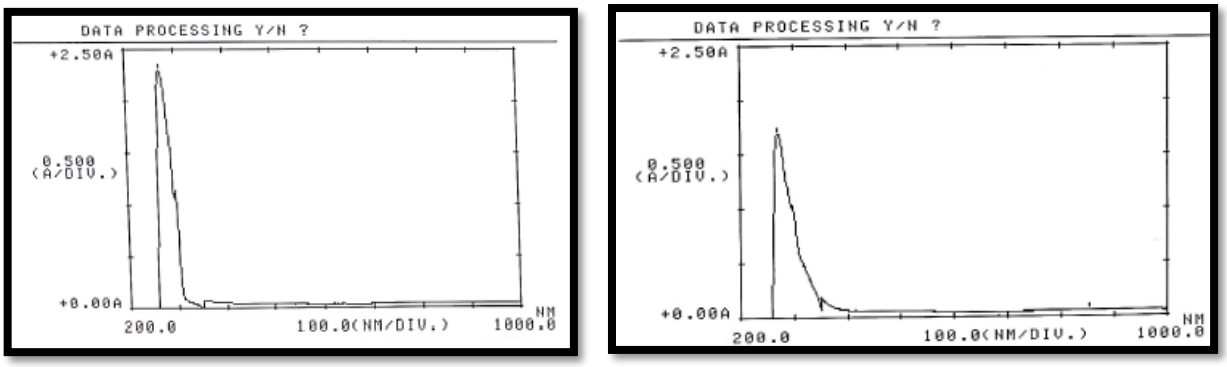

(A) (B)

Fig. 6: Electronic spectrum of the L^1 (A) and Cu-complex (B)

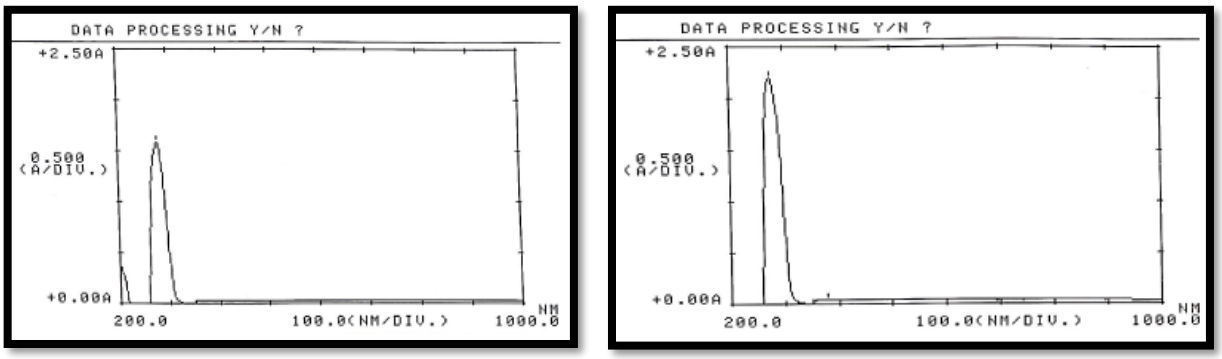

(A) (B)

Fig. 7: Electronic spectrum of the L^2 (A) and Cd-complex (B)

Magnetic moments and Conductivity measurements

In table 8 and 9, values of the measured magnetic susceptibility and effective magnetic moment (μeff) for Mn (II), Ni(II), Co(II), and Cu(II) complexes have been shown. Those complexes exhibit μeff (6.04, 3.87, 4.71, and 2.26) B.M respectively of L^1 and μeff (5.71, 3.68, 4.49, and 2.19) BM respectively of L^2 those normal values had been found to be consistent with the high spin tetrahedral complex types. Non- electrolytes nature of all metal complexes has been confirmed by measurements of the molecular conductivity [35,36].

Cell Viability and Cytotoxicity Assays

Based upon tetra-solium salt - (4,5-dimethyl-thiazol-2yl)-2,5-di-phenyltetrazo-lium bromide (MTT), the cytotoxicity has been measured by the colorimetric assay. On protocol which has been first described in 1983 by T. Mossman, MTT testing has been adopted in anti-cancer activities. MCF7 tumor cell lines have been compared to normal (HdFn) cell line that has been utilized in the present work. At concentration levels that range from between 25 µg / mL and 400µg / mL of $[Cu_2(L^1)Cl_4]$ and $[Co_2(L^1)Cl_4]$, the MCF7 cell line and normal cell line (HdFn) were exhibited.

In order to clarify the effect of $[Cu_2(L^1)Cl_4]$ and $[Co_2(L^1)Cl_4]$ complexes on the cancerous and normal cell types, it has been noticed that the maximum cell growth inhibition rate has been at (25µg/ml) and lowest cell growth inhibition rate has been at (400µg\ml) for concentrations of the breast cells MCF-7 and the normal cells (HdFn) [37,38].

Based on cell line type, rates of $[Cu_2(L^1)Cl_4]$ and $[Co_2(L^1)Cl_4]$ inhibition will vary between (95.71 - 33.95)% and (95.94 – 54.08)% for the MCF-7 breast cancer cell line and (94.25 – 66.74)% and (95.21 – 76.04)% for normal (HdFn) cell line, had specified the number of live cells that remain after the interaction with $[Cu_2(L^1)Cl_4]$ and $[Co_2(L^1)Cl_4]$ complexes respectively. An important result that must be obtained by tests of the MCF-7 cancer cell lines is (IC-50) (inhibitor Concentration 50), and in turn, this concentration kills about 50% of cells, table10.

The half inhibitor equals (121.7µg/ml) and (148.5µg/ml) in a case of interaction of Cu and Co complexes respectively with the MCF-7 breast cancer cell line. When comparing the complexes in terms of half inhibitory concentration (IC50), it was found that the best complex used as an anti-cancer treatment among the complexes is the copper complex because it has an effective toxic effect against the cells of breast cancer cell line (MCF7). It is higher than the cobalt complex because it kills almost half of the cancer cells and is less toxic to normal cells than the cobalt complex [39,40], figure 8 (A,B).

Table 10: The effect of $[Cu_2(L^1)Cl_4]$ and $[Co_2(L^1)Cl_4]$ on breast cancer cell line (MCF7) and in comparison to normal cell line at same concentration utilizing the MTT test for a 24 hour period At 37°C temperature

Concentration µg mL^{-1}	Mean viability (%) ± SD Cu-complex		Mean viability (%) ± SD Co-complex	
	HdFn	MCF-7	HdFn	MCF-7
400	66.74±2.9	33.95±4.14	76.04±1.97	54.089±2.56
200	75.57±2.20	46.103±4.68	86.26±2.38	65.239±4.9
100	87.15±1.10	68.78±4.029	85.957±3.12	84.72±1.3
50	94.09±0.50	78.74±7.02	93.94±0.066	94.29±0.820
25	94.25±1.3	95.717±0.8	95.216±0.65	95.949±0.90

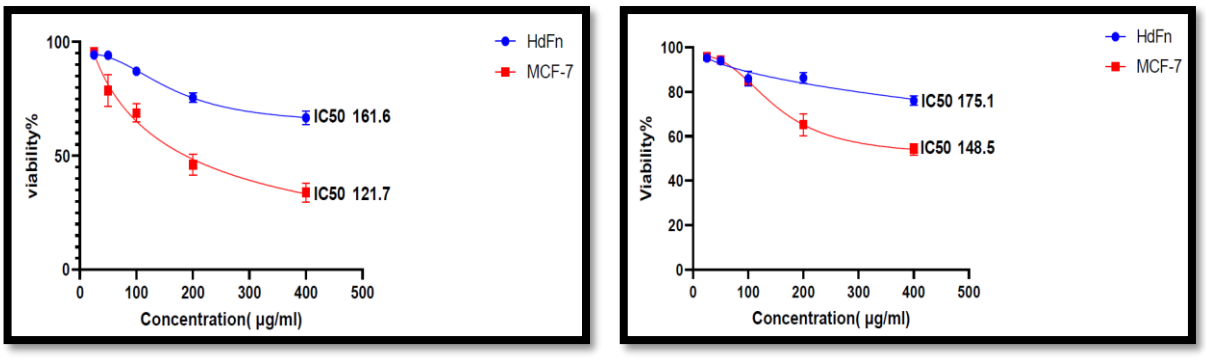

(A) **(B)**

Fig. 8: shows the relation between vital activity of breast cancer line (MCF7) and normal cells (HdFn) with $[Cu_2(L^1)Cl_4]$ (A) and $[Co_2(L^1)Cl_4]$ (B) in different concentrations

Studies of the Antibacterial Activity

S. aureus (G+) and E. coli (G-) have been utilized as testing organisms. To conduct the assay on test organisms, medium surface has been inoculated as well as covered. Allow agar surface to dry for 3min-5min before inserting disks. With the use of sterile forceps, tablets have been dipped in chemical beaker, then inserted into the medium. The bacteria plates were incubated for a period of 48 hrs. at 37 ° C to proliferate. Complexes exhibit varying levels of activity in the limiting of bacteria's proliferation when compared with the ligand (P) concentration levels [41,42]. The results are detailed in figure 9 (A,B), table 11.

Table 11: Results that have been obtained from biological activities of prepared complexes.

No.	Compound	E. coli	S. aureus
1	DMSO	0	0
2	L^1	0	10
3	L^2	0	10
4	A_2 / $[Cu_2(L^1)Cl_4]$	13	12
5	B_5 / $[Mn_2(L^2)Cl_4]$	8	11

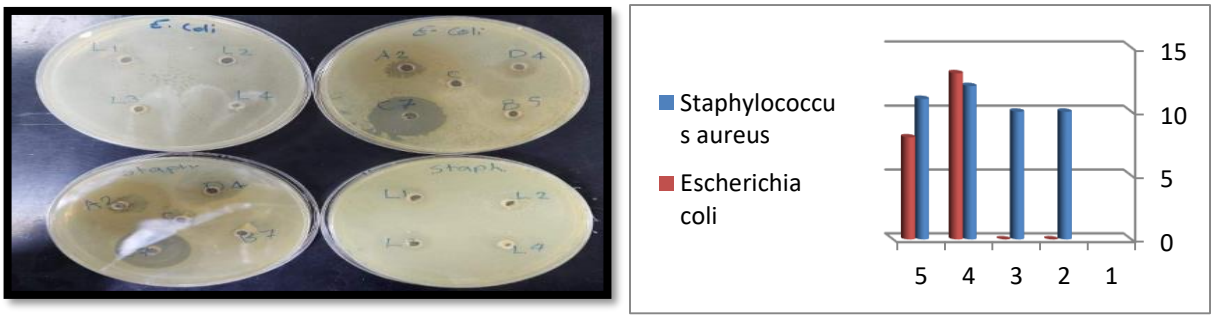

Fig. 9: Figure of biological activity of prepared complexes (A)
Graph of bio-activity results of prepared complexes (B)

Thermal analysis

Ligands (L^1 & L^2) have been prepared as well as subjected to a thermal analysis process utilizing a STAPT-1000 device made by the German company Linseis. This measurement was carried out in an environment of argon gas at a 10°C/min heating rate with 0°–

700°C temperature range [43,44]. Any results that were reported come from the TG curves for ligands (L^1 and L^2) that were studied in table 12, figure 10 (A,B)

Table 12: Temperature degrees for analyses along corresponding values of weight loss.

Ligands	Stage	TGA			DSC	
		TG range(˚C)	%Estimated (calculated) Mass loss	Assignment	T(˚C)	Peak
L^1	1	50-137	0.3464(0.3391)	- O_2 ,$3H_2$	132.28	endo
	2	138-280	1.7450(1.7409)	- 3S ,1C, $3/2H_2$	137.8	exo
	3	281-600	1.7975(1.8471)	- 1S , $7/2H_2$,14C		
L^2	1	50-120	0.2676(0.3101)	-N_2	80.36	endo
	2	121-295	3.7170(3.7051)	-N_2,O_2,2S,16C,$9H_2$	91.34	exo
	3	296-600	0.5522(0.5547)	-4C,H_2	155.04	exo
					177.04	endo
					231.61	exo
					256.44	endo

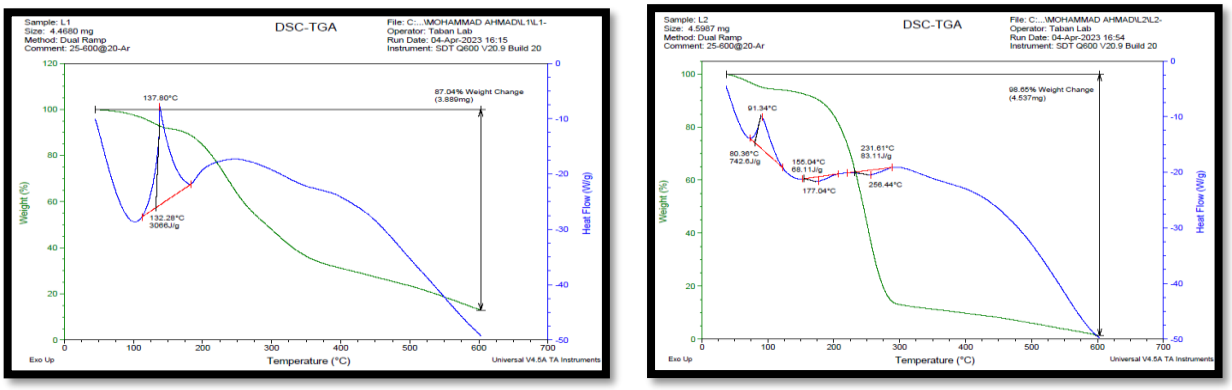

(A) (B)

Fig. 10: Thermal study of L^1 (A) and L^2 (B)

Conclusion

This investigation involved the characterization and synthesis of seven complexes for each of the ligands L1 and L2, which are produced by reacting succinyl chloride with 2-aminobenzothiazole or benzylamine, respectively. Transition metal ions, including Ni(II), Mn(II), Cu(II), Co(II), Zn(II), Cd(II), and Hg(II), are used in this study. The bidentate ligands (L1 and L2) are found to be potent donors, with the (C=S) and (C=O) groups serving as the ligands. The anti-microbial activity of both ligands and their complexes are tested against two different bacterial species. Additionally, the anti-cancer activity of $[Cu_2(L1)Cl_4]$ and [Co2(L1)Cl4] complexes are evaluated using MCF7-type breast cancer cell lines, and the results are compared to those obtained from normal cell lines in a cell cytotoxicity and viability assay. These complexes may have potential as drugs for treating various malignant disorders that affect humans.

References

1. Bożena Kuran, Jerzy Kossakowski and Mariola Krawiecka, Synthesis and biological activity of novel series of heterocyclic compounds containing succinimide moiety, Heterocycl. Commun. 2013; 19(4): 287–296
2. Osama'a A.Y. Al-Samrai ,Synthesis, characterization and bioactivity evaluation of zinc(II) and cadmium(II) complexes with some non-steroidal antiinflammatory drug ligands, Samarra J. Pure Appl. Sci., 2022; 4 (4): 1-16.
3. Larisa V. Zhilitskaya, Nina O. Yarosh, Synthesis of biologically active derivatives of 2-aminobenzothiazole, Chemistry of Heterocyclic Compounds, 2021, 57(4), 369–373
4. J. Joseph, G. Boomadevi Janaki and J. Dharmaraja, Metal complexes of 2–aminobenzothiazole derivatives as a versatile system tuning up their structural and biological properties,J. Chem. Pharm. Res., 2016, 8(1S):133-152.
5. Ivana Šagud, Nikolina Maček Hrvat, Ana Grgičević, Design, synthesis and cholinesterase inhibitory properties of new oxazole benzylamine derivatives, Journal of Enzyme Inhibition and Medicinal Chemistry 2020, vol. 35, NO. 1, 460–467.
6. Søren Kramer, Synthesis of α-Substituted Primary Benzylamines through Copper-Catalyzed Cross-Dehydrogenative Coupling,Org. Lett. 2019, 21, 1, 65–69.
7. Basima M. Sarhan, Sajid M. Lateef and Enass J. Waheed, Synthesis and Characterization of Some Metal Complexes of [N-(1,5-dimethyl-3-oxo-2-phenyl-2,3-dihydro-1H-pyrazol4-ylcarbamothioyl) acetamide], Ibn Al-Haitham Journal For Pure And Applied Science, 2015, 28(2),102-115.
8. Basima M. Sarhan,Nada J. Kadhim and Enass J. Wheed, Stability constant of some Metal Ion Complexes of (6-(2- Amino-2-(4-hydroxy phenyl)-acetamido)-3,3- -dimethyl-7-oxo-4-thia-1-aza-bicyclo[3,2,0]heptanes-2- carboxylicacid (Amoxicillin), Ibn Al-Haitham Journal For Pure And Applied Science,2013,vol. 26 (3),p.245-253.
9. Awf A.R. Ahmed and Enass J. Waheed, “Synthesis, Characterization, Thermal Study, Biological Activity and Corrosion Inhibition of New Ligand Derived from Butanedioyl Dichloride and Some Selective Transition Metal Complexes” Journal of Global Pharma Technology 2019: vol11.pp379-391.
10. Taghreed Q. Abd Alkareem and Enass J. Waheed, Formation, Characterization and Antioxidant Study of Mixed Ligand Complexes Derived from Succinyl Chloride,chem.methodol. 2022, 6(12),914-928.
11. Sunjuk, Mahmoud, et al. "Transition Metal Complexes of Schiff Base Ligands Prepared from Reaction of Aminobenzothiazole with Benzaldehydes." Inorganics 2022: 10.4, 43.
12. Miami H. Ali and Eman Abdul Wahid Othman, Synthesis, characterization and evaluation of the bacterial activity of complexes of some transition metals containing Benzimidazole derivatives, Samarra J. Pure Appl. Sci., 2021; 3 (1): 25-36 .
13. Bepary, S., et al. "N-acetylation of 2-aminobenzothiazoles with Acetic Acid for Evaluation of Antifungal Activity and In Silico Analysis." Journal of Molecular Docking 1.2, 2021: 78-83.
14. Alminderej, F. et al. "Design, Synthesis, Characterization and Anticancer Evaluation of Novel Mixed Complexes Derived from 2-(1H-Benzimizadol-2-yl) aniline Schiff base and 2-Mercaptobenzimidazole or 2-Aminobenzothiazole. " Egyptian Journal of Chemistry 64.7, 2021: 3351-3364.

15. Yagüe, C., et al. "Non-emissive RuII Polypyridyl Complexes as Efficient and Selective Photosensitizers for the Photooxidation of Benzylamines." Chemistry–A European Journal 26.53 , 2020: 12219-12232.
16. Dong, C., et al. "4, 6-Dihydroxysalicylic Acid-Catalyzed Oxidative Condensation of Benzylic Amines and Aromatic Ketones for the Preparation of 2, 4, 6-Trisubstituted Pyridines and Its Application to Metal-Free Synthesis of G-Quadruplex Binding Ligands." ACS omega 4.5 2019: 9029-9040.
17. Joseph, K. et al. "Metal complexes of 2-aminobenzothiazole derivatives as a versatile system tuning up their structural and biological properties." J. Chem. Pharm. Res 2016,8: 133-152.
18. Ahmed, K., et al. "Synthesis, Characterization and Biological Activity Evaluation of Some New Azo Derivatives from 2-Amino Benzothiazole and Their Derivatives." Kirkuk University Journal-Scientific Studies, 2018, 13.1: 212-227.
19. Jin, J., et al. "Iridium complexes containing bis (imidazoline thione) and bis (imidazoline selone) ligands for visible-light-induced oxidative coupling of benzylamines to imines." Organometallics, 2013, 32.14: 3954-3959.
20. Karami, K., et al. "Synthesis and structural studies of cyclopalladated complexes of secondary benzylamines." Journal of Organometallic Chemistry, 2013, 728: 16-22.
21. Ibrahim, S., et al. "Newly synthesized benzothiazole derived ligand and its Co (III) and Ru (III) complexes as biological potent molecules: Chemical preparation, structure, antimicrobial, in vitro and in vivo cytotoxicity studies." Biointerface Res Appl Chem 12, 2022: 7817-7844.
22. Ravichandran, K., et al. "(Benzylamine) chloridobis (ethane-1, 2-diamine) cobalt (III) dichloride hemihydrate." Acta Crystallographica Section E: Structure Reports Online, 2009, 65.10: m1174-m1175.
23. Ilkimen, M., et al. "Synthesis, characterization, and pharmacological evaluation of the proton transfer salts of 2-aminobenzothiazole derivatives with 5-sulfosalicylic acid and their Cu (II) complexes." Journal of Coordination Chemistry 71.16-18, 2018: 2831-2842.
24. Suh, S. et al "Bis (2-aminobenzothiazole-κN1) bis (thiocyanato-κN) zinc (II)." Acta Crystallographica Section E: Structure Reports Online, 2009, 65.9: m1054-m1054.
25. Cabeza, J., et al. "(Benzylamine-N)(η5-cyclopentadienyl) bis (triphenylphosphine-P) ruthenium (II) tetrafluoroborate." Acta Crystallographica Section E: Structure Reports, 2001: m162-m163.
26. Zalevskaya, O., et al. "Chiral palladium complexes based on derivatives of benzylamine and 2α-hydroxypinan-3-one." Natural Science 2.11, 2010: 1189.
27. Harshita, P., et al. "Design Synthesis and Biological Evaluation of Dithiocarbamate Substituted 2-Aminobenzothiazole Derivatives as Proviral Integration Site of Moloney Murine Leukaemia Virus 1 Kinase Inhibitors." Indian Journal of Pharmaceutical Sciences, 2020, 82.6: 1015-1024.
28. Zalevskaya, O., et al. "Chiral palladium complexes based on derivatives of benzylamine and 2α-hydroxypinan-3-one." Natural Science 2.11, 2010: 1189.
29. Kyhoiesh, H. et al, "Synthesis, spectral characterization and biological activities of Ag (I), Pt (IV) and Au (III) complexes with novel azo dye ligand (N, N, O) derived from 2-amino-6-methoxy benzothiazole." Chemical Papers, 2022: 1-34.
30. Dadmal, T. et al, Contemporary progress in the synthesis and reactions of 2-aminobenzothiazole: a review, New Journal of Chemistry, 2017,1-22.

31. Ulviye A., et al, Synthesis of new benzothiazole derivatives bearing thiadiazole as monoamine oxidase inhibitors, J Heterocyclic Chem. 2020;1–9.
32. Søren K., Synthesis of α-Substituted Primary Benzylamines through Copper-Catalyzed Cross-Dehydrogenative Coupling,Org. Lett. 2019, 21, 1, 65–69.
33. Ivana Š., et al, Design, synthesis and cholinesterase inhibitory properties of new oxazole benzylamine derivatives, Journal of Enzyme Inhibition and Medicinal Chemistry 2020, vol. 35, NO. 1, 460–467.
34. Wisam A., et al. "Metal complexes of ligand derived from amine compound: formation, spectral characterization and biological evaluation." International Journal of Drug Delivery Technology, 2021:vol 11.pp728-734.
35. Willis J. B. and Mellor D. P., The Magnetic Susceptibility of Some Nickel Complexes in Solution, J. Am. Chem. Soc. ,1947, 69, 6, 1237–1240.
36. Revanasiddappa, M., et al, Electrical Conductivity Studies on Co(II), Cu(II), Ni(II) and Cd(II) Complexes of Azines,Journal of Chemistry,2008, Vol. 5, No.4, pp. 797-801.
37. Paynter, D. et al. Changes in activity of the Cu-Zn superoxide dismutase enzyme in tissues of the rat with changes in dietary copper. The Journal of nutrition, 1979, 109(9), 1570-1576.
38. Campbell, V., et al. Pharmacokinetic and anti-cancer properties of high dose ascorbate in solid tumours of ascorbate-dependent mice. Free Radical Biology and Medicine, 2016, 99, 451-462.
39. Calabrese, S., et al. Evidence for hormesis in mutagenicity dose–response relationships. Mutation Research/Genetic Toxicology and Environmental Mutagenesis, 2011, 726(2), 91-97.
40. Arshad, N., et al. Peganum harmala can minimize Escherichia coli infection in poultry, but long-term feeding may induce side effects. Poultry science, 2008, 87(2), 240-249.
41. Juber, A., et al. "Design, Synthesis, Characterization and Biological Evaluation of 6-Methoxy-2-aminobenzothioate derivatives against certain bacterial strains." Egyptian Journal of Chemistry 63.10, 2020: 3891-3901.
42. Khalil, M., and Khalal. Q. "Synthesis and characterization of new compounds derived from 2-hydrazinobenzothiazole and evaluated their antibacterial, Journal of Physics: Conference Series, 1853 012007, 2021, 1-14.
43. Bozza, G., et al., Claudia, Eduardo Tonon. Synthesis and thermal behavior study of complexes of the type $[Pd(\mu\text{-}X)(4\text{-eb-p-phen})]_2$ (X = Cl, Br, I, N_3, NCO, SCN) and 4-eb-p-phen [bis(4-ethylbenzyl)p-phenylenediimine]. Journal of Thermal Analysis and Calorimetry, 2014 118(1), 67–74.
44. Wenkin, M., et al. "Diammine (pyrazine-2, 3-dicarboxylato-N, O) palladium (II): synthesis, crystal structure, spectroscopic and thermal properties." Inorganica chimica acta 258.1 ,1997: 113-118.

IRAQI Academic Scientific Journals
Samarra Journal of Pure and Applied Science
SJPAS
مجلة سامراء للعلوم الصرفة والتطبيقية
www.sjpas.com
p ISSN: 2663-7405
e ISSN: 2789-6838

معقدات فلزية قائمة على ليكاند جديد: تحضير، تشخيص طيفي، سلوك حراري، خصائص مضادة للسرطان والفعالية البيولوجية

محمد احمد مضحي[1]، ايناس جاسم وحيد[2*]، مها صالح حسين[2]

1 قسم الكيمياء، كلية التربية، جامعة سامراء، سامراء، العراق

2 قسم الكيمياء، كلية التربية للعلوم الصرفة/ابن الهيثم، جامعة بغداد، بغداد، العراق

معلومات البحث:

تأريخ الاستلام: 2023/04/27

تأريخ القبــول: 2023/05/31

الكلمات المفتاحية:

N^1,N^4- ثنائي كاربامو ثايويل سكسناميد, 2-امينو بنزوثايازول, بنزايل امين

معلومات المؤلف

الايميل:

الموبايل:

الخلاصة:

ليكاندات جديدة، N1, N4-bis(benzo[d]thiazol-2- ylcarbamothioyl) succinamide (L^1) and N1, N4- bis (benzylcarbamo thioyl) succinamide (L^2) مشتقة من كلوريد السكسنيل و 2-امينوبنزوثايوزول او البنزايل امين على التوالي لتحضير مجموعة من المعقدات الفلزية ذات الصيغة العامة$[M_2(L)Cl_4]$ ، حيث $L=L^1$ or L^2, M = Mn(II), Ni(II), Cu(II), Cd(II), Co(II), Zn(II) or Hg(II)، تم تشخيص المركبات المحضرة باستخدام تقنيات تحليلية مختلفة بما في ذلك التحليل الحراري وطيف الرنين النووي البروتوني والكاربوني وطيف الكتلة والاشعة تحت الحمراء والقياسات المغناطيسية والتوصيلية المولارية والتحليل الدقيق للعناصر والامتصاص الذري. حيث أظهرت النتائج أن (L^1,L^2) ترتبط بأيون الفلز بطريقة ثنائية السن من خلال مجموعتي (C=O) و (C=S)وأن المعقدات لها شكل هندسي رباعي السطوح. تم اختبار النشاط المضاد للبكتيريا للمركبات ضد نوعين من البكتيريا، الإشريكية القولونية (-) والمكورات العنقودية الذهبية (+). بالإضافة إلى ذلك، تم تقييم النشاط المضاد للسرطان لمعقدي Cu (II)و Co (II) من خلال إجراء فحوصات بقاء الخلية والسمية الخلوية على خط خلايا سرطان الثدي MCF-7 ومقارنة النتائج مع تلك التي تم الحصول عليها للخلايا الطبيعية.